Coring and Segregation

Lesley Cornish

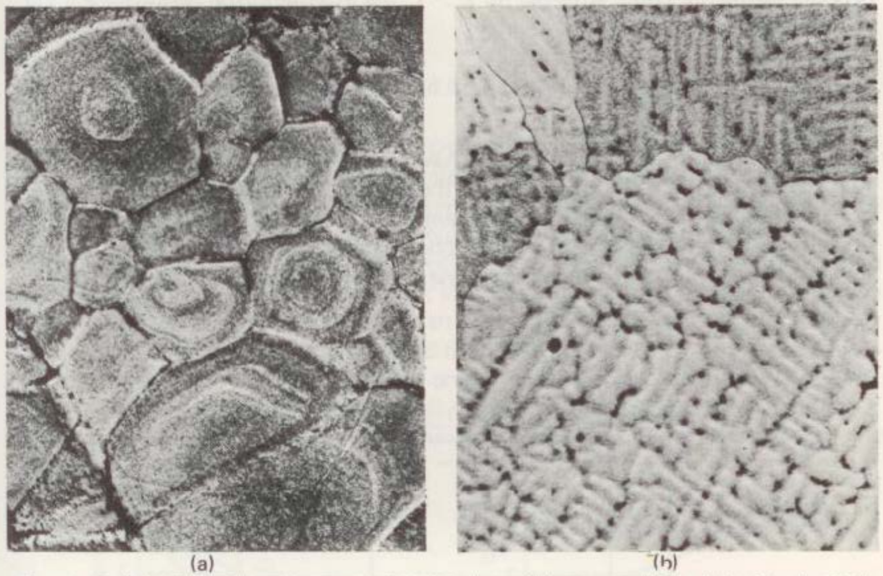

Figure 4.8 *(a) Spherical coring pattern in a zinc-based alloy containing zirconium (× 400). (b) Example of the usually observed cored dendritic morphology in impure metals and alloys, showing interdendritic segregation, porosity, and grain boundary pinning (× 100)*

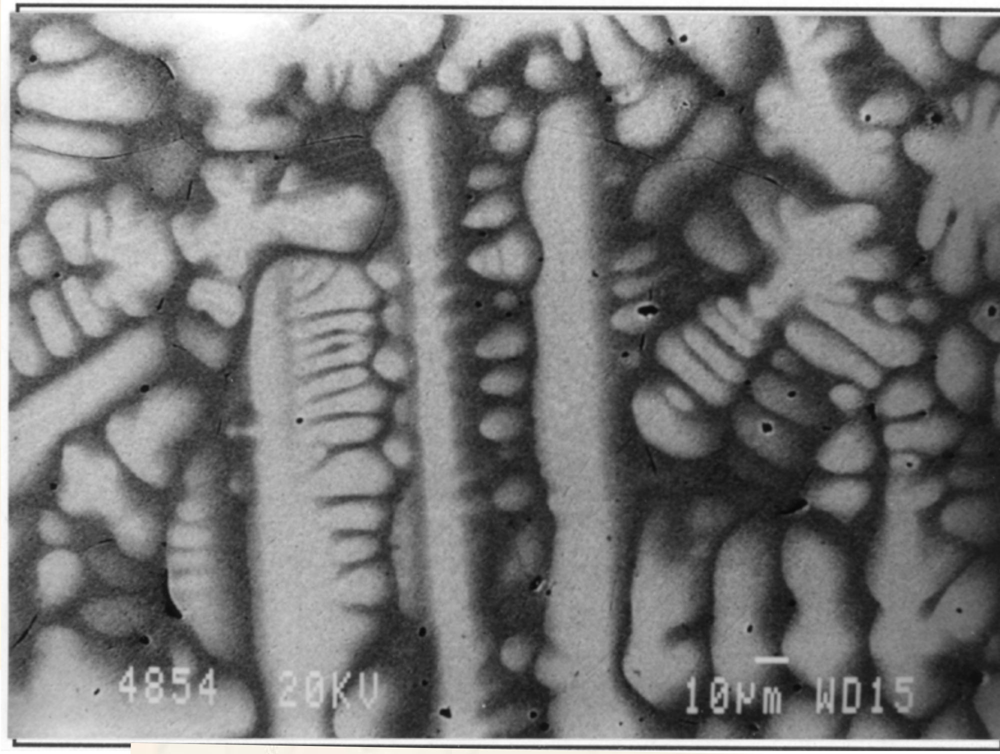

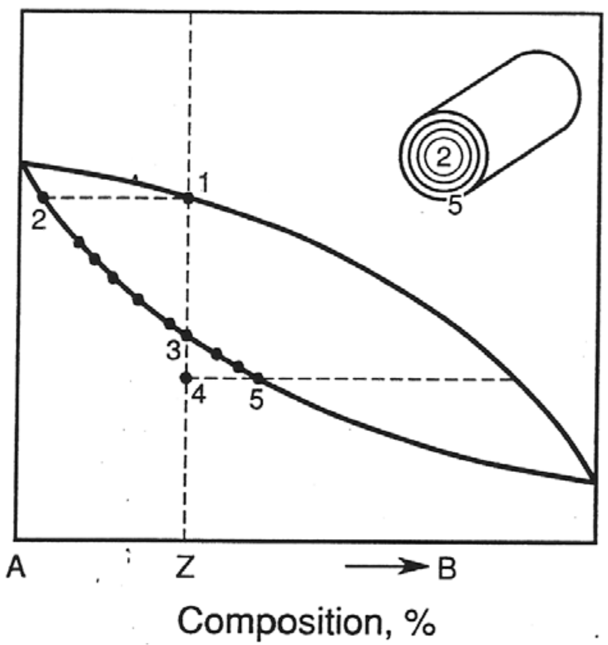

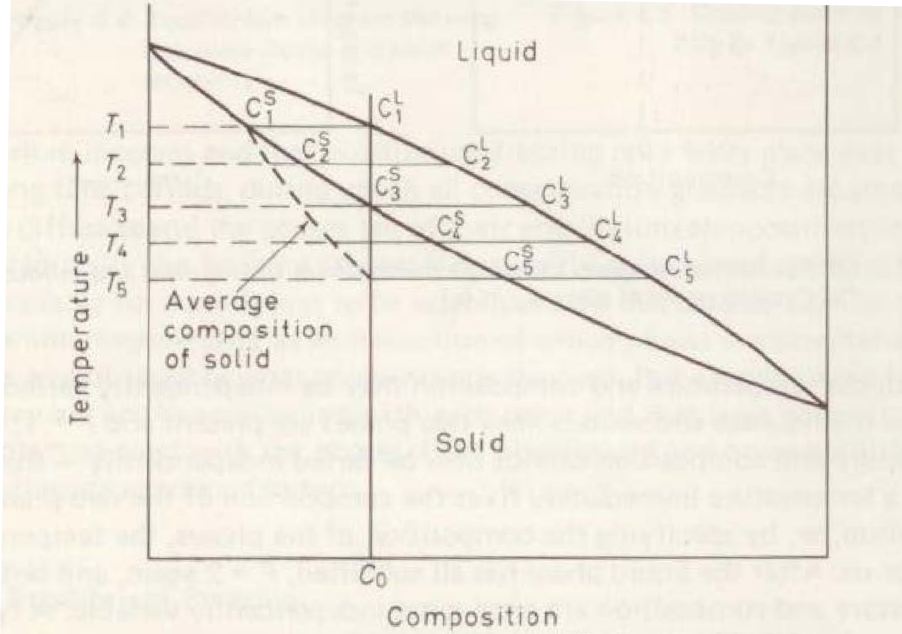

Figure 4.7 *Equilibrium diagram and non-equilibrium freezing isotherms*

Showing a diffuse boundary between coring, and a "hard boundary" between the phases

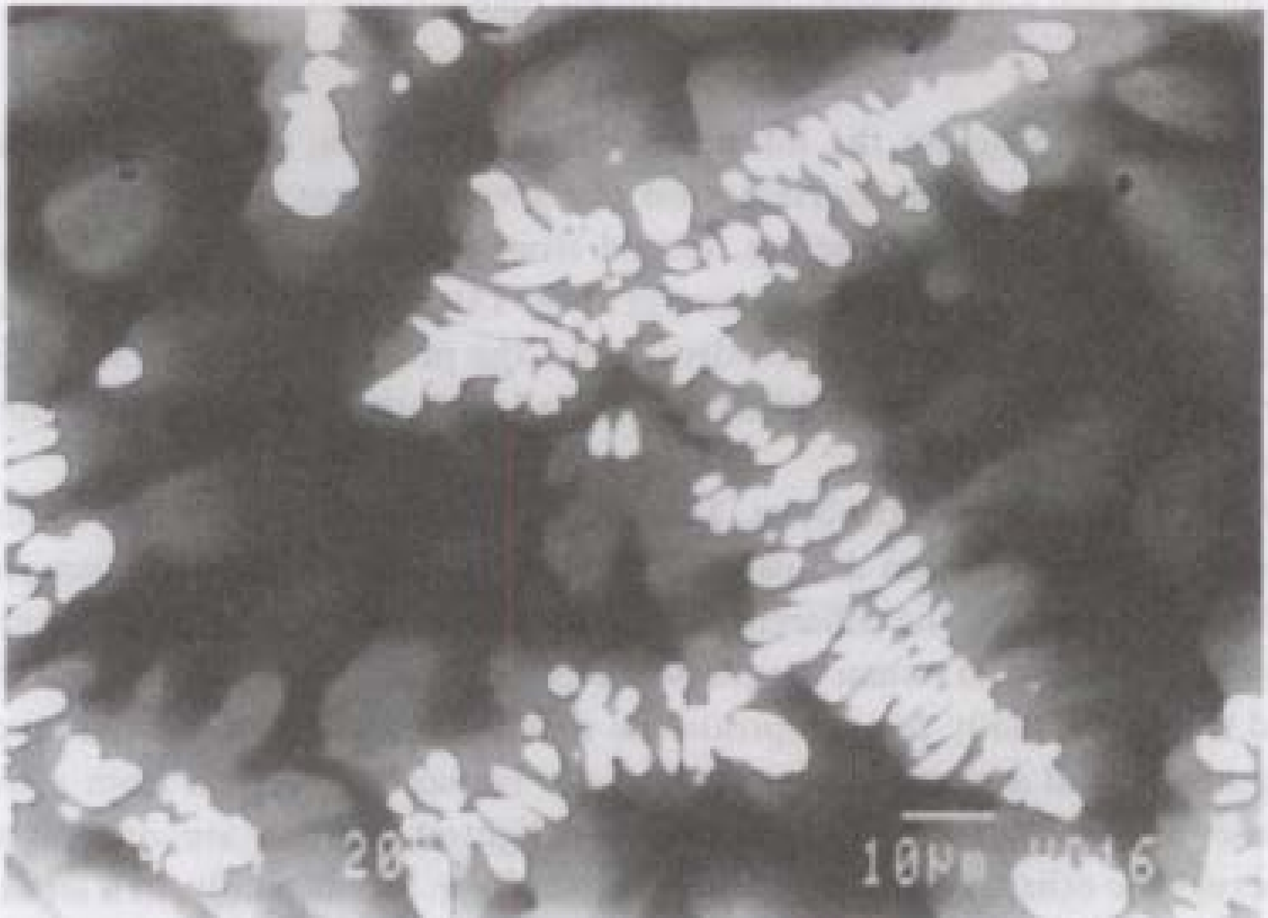

FIGURE 15 SEM image in backscattered electron mode. Al – 76 (at.%) Ni – 9 Re alloy showing the difference between coring and a separate phase. (Re) dendrites (light) with cored (Ni) (medium to dark grey) [34].

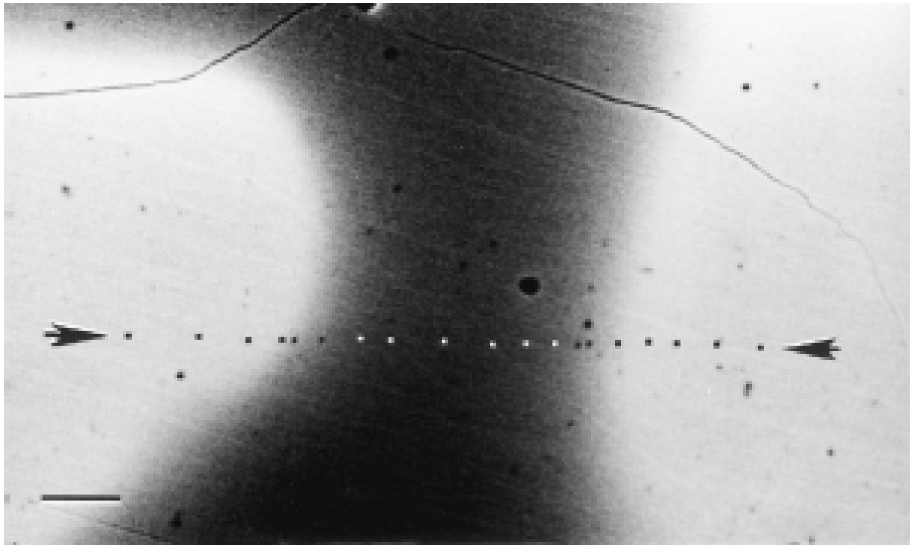

Fig. 4. $Al_{43}Ni_{43}Ru_{14}$: SEM image in backscattered mode showing the locations analysed across the microsegregation. Annealed at 1600 °C for 12 h and furnace cooled. Bar represents 10 μm.

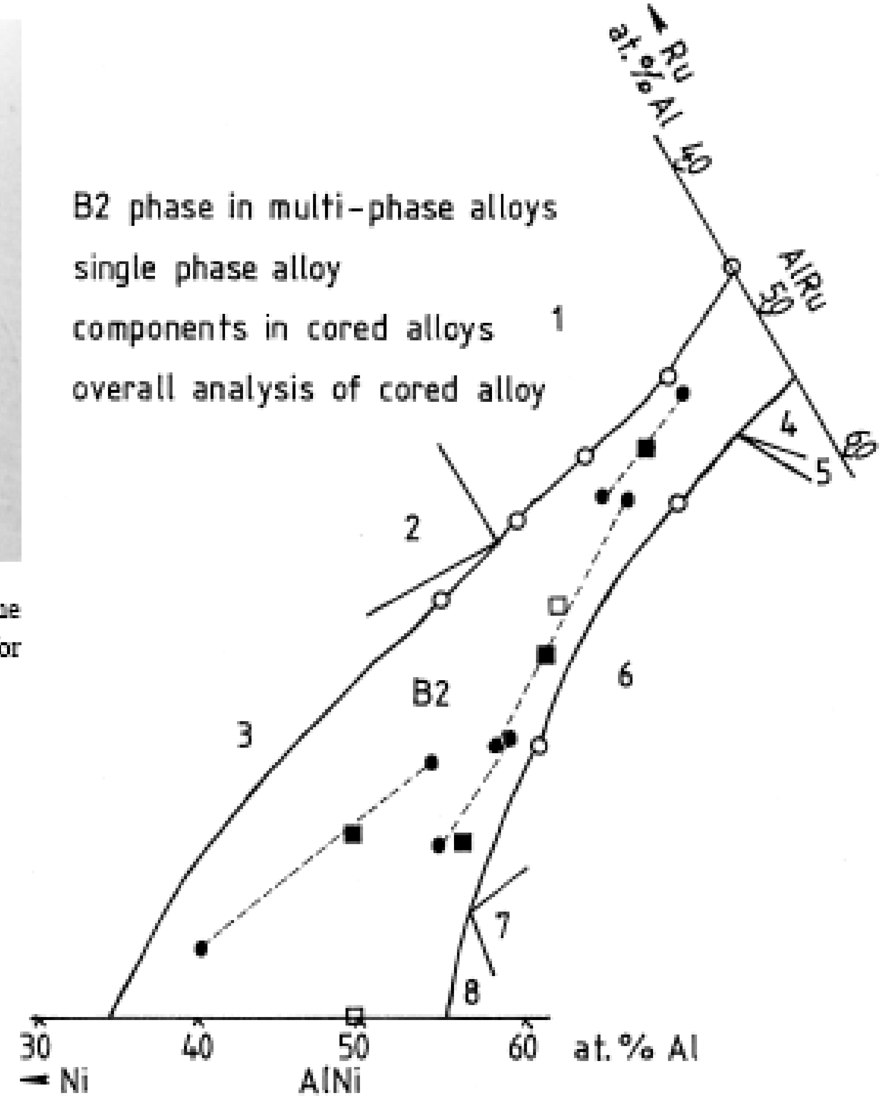

Fig. 5. Compositions of the B2 phase obtained from EDS analysis, including analyses of multi-phase alloys reported elsewhere [18–20]. Samples were annealed at 1500 °C or 1600 °C for 12 h and then furnace cooled. Key to numbered regions: 1, B2 + (Ru); 2, B2 + (Ru) + $AlNi_3$; 3, B2 + $AlNi_3$; 4, B2 + Al_3Ru_2; 5, B2 + Al_3Ru_2 + Al_2Ru; 6, B2 + Al_2Ru; 7, B2 + Al_2Ru + Al_3Ni_2; 8, B2 + Al_3Ni_2.

Coring because:
Overlapping compositions
XRD peaks between NiAl and RuAl.

Other workers only looked at two alloys

Fe – C system

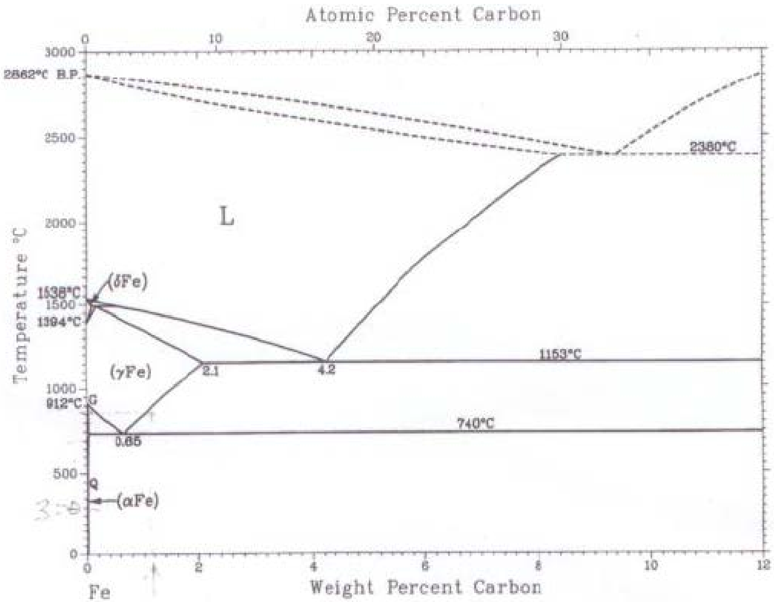

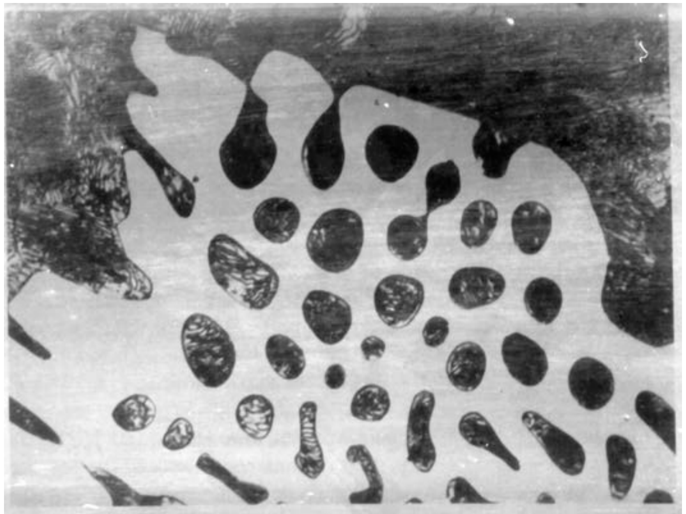

Fig. 121. Some pearlite in the ledeburite is resolved as well. 1000x.

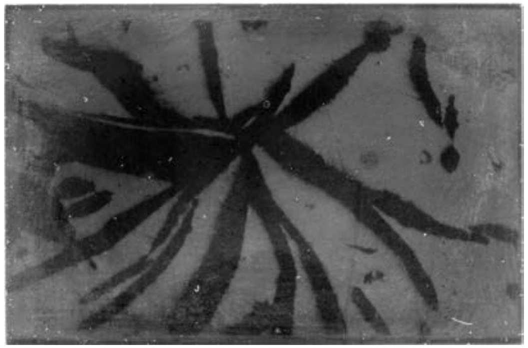

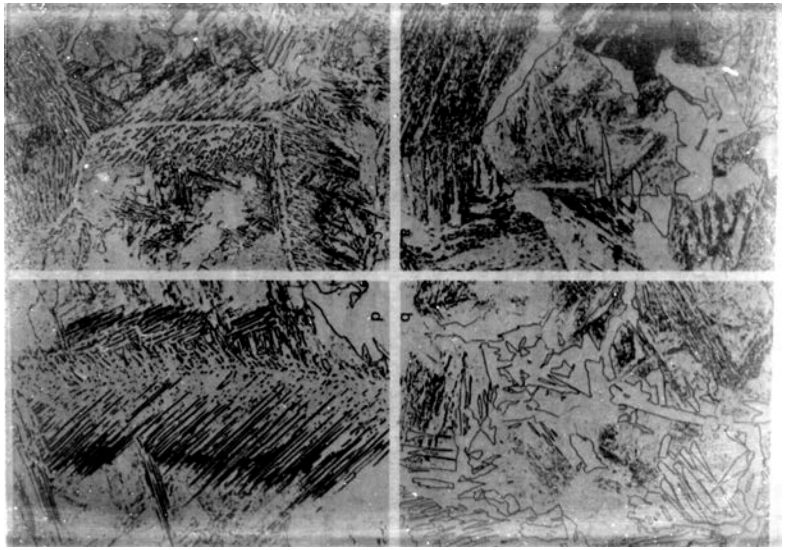

Figure 4.66 Scanning electron micrograph of flake graphite in cast iron, showing the gross distortion and the interconnected nature of the graphite (× 5000) (Courtesy of M. G. Day, B.C.I.R.A.)

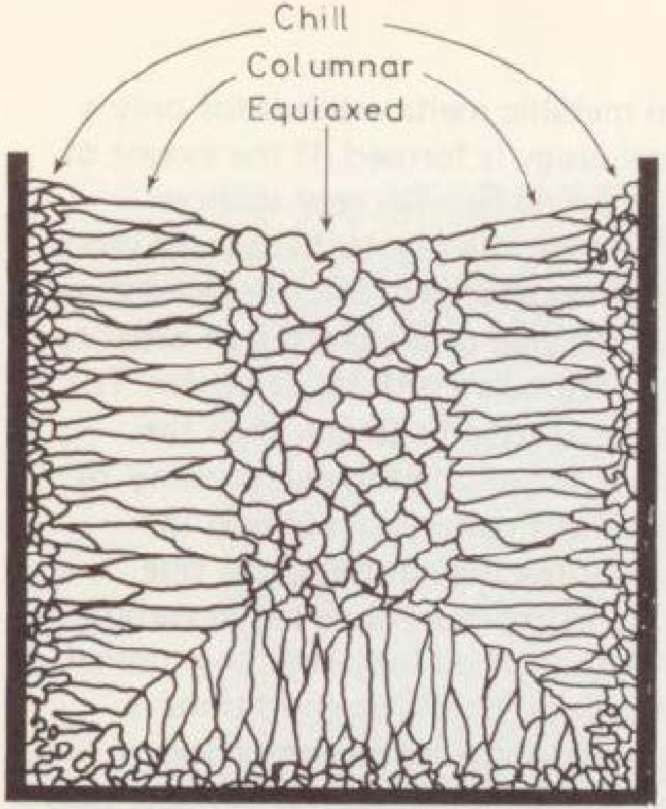

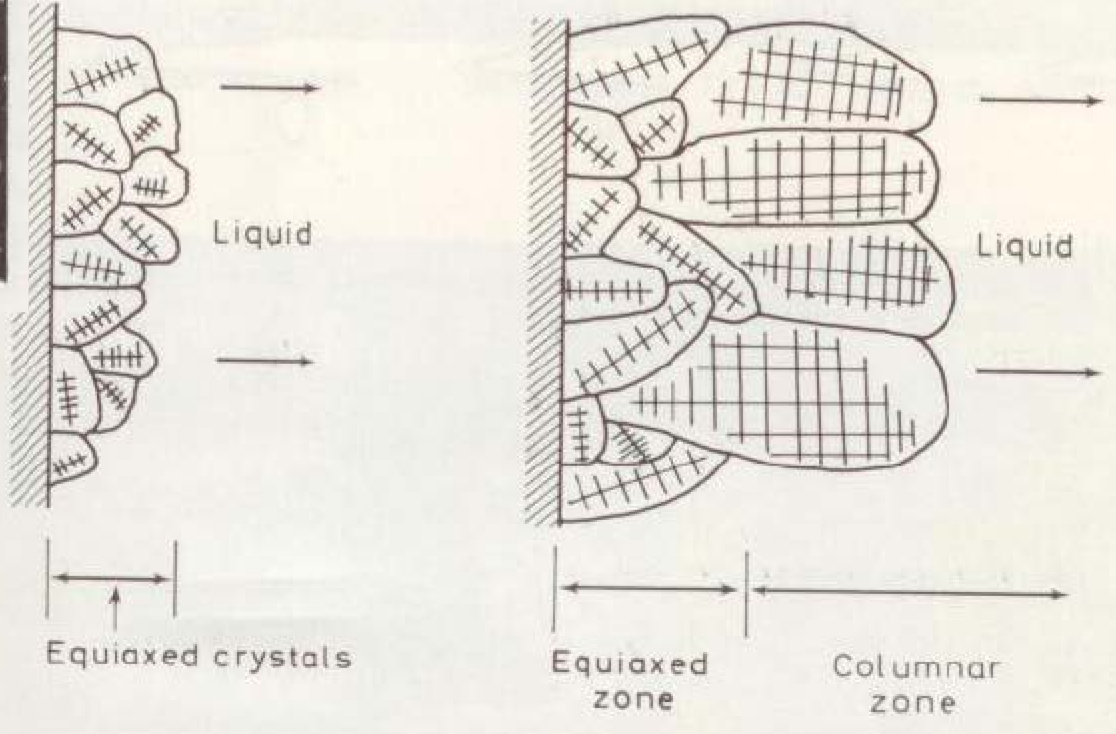

Figure 4.24 Schematic drawing illustrating the growth of the columnar grains from favourably orientated grains in the chill zone

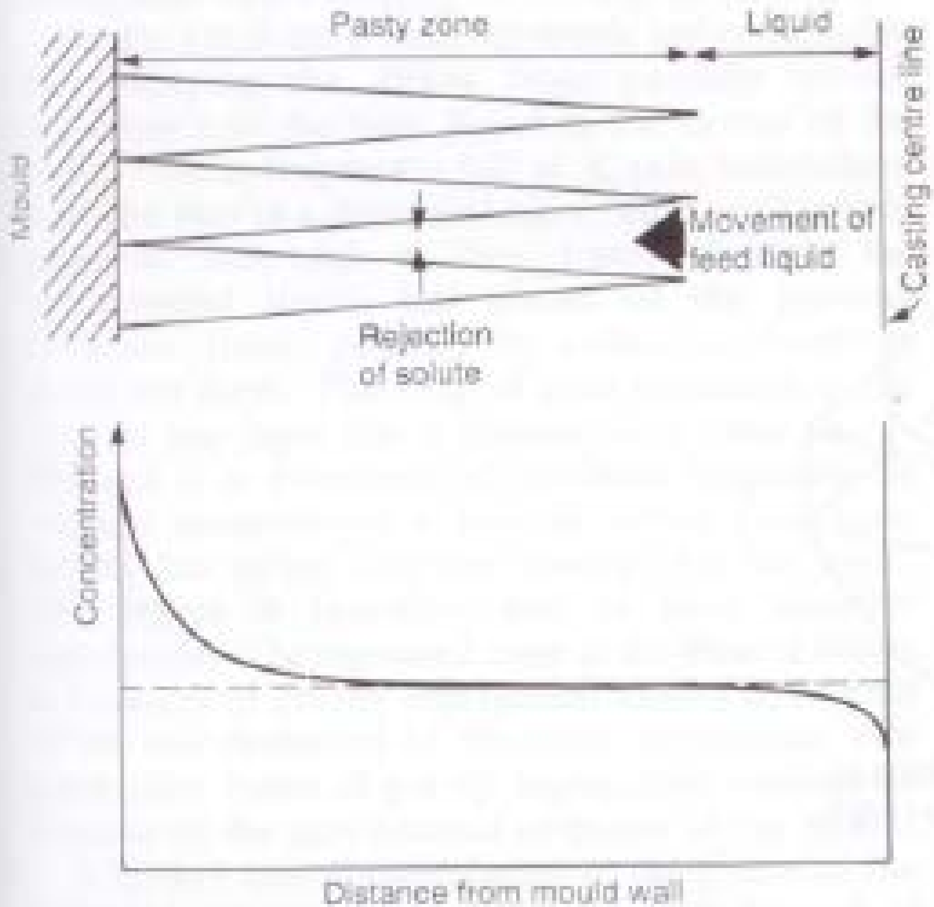

Figure 4.34 *Normal dendritic segregation (usually misleadingly called inverse segregation) arising as a result of the combined actions of solute rejection and shrinkage during solidification in a temperature gradient.*

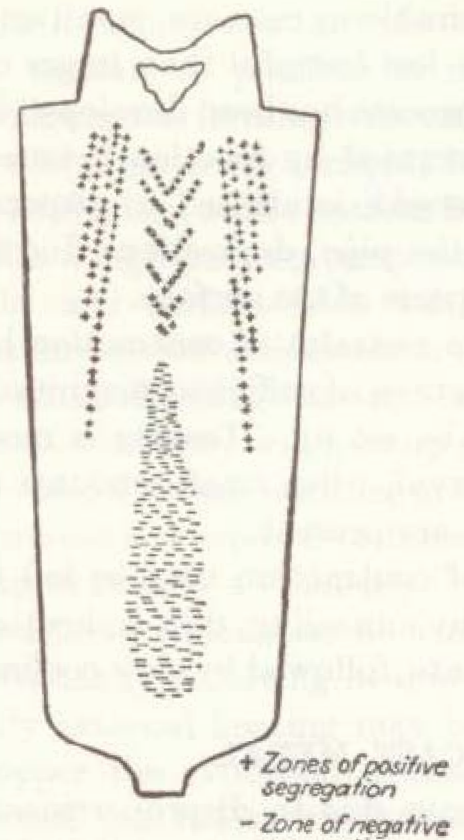

FIG. 289. Segregation in killed steel ingot. The central and outer regions of positive segregation are often referred to as the V and Λ segregates, respectively. The degree of segregation of the principal constituent elements is in the following order: sulphur, (phosphorus, carbon), silicon, manganese. From J. W. Halley.

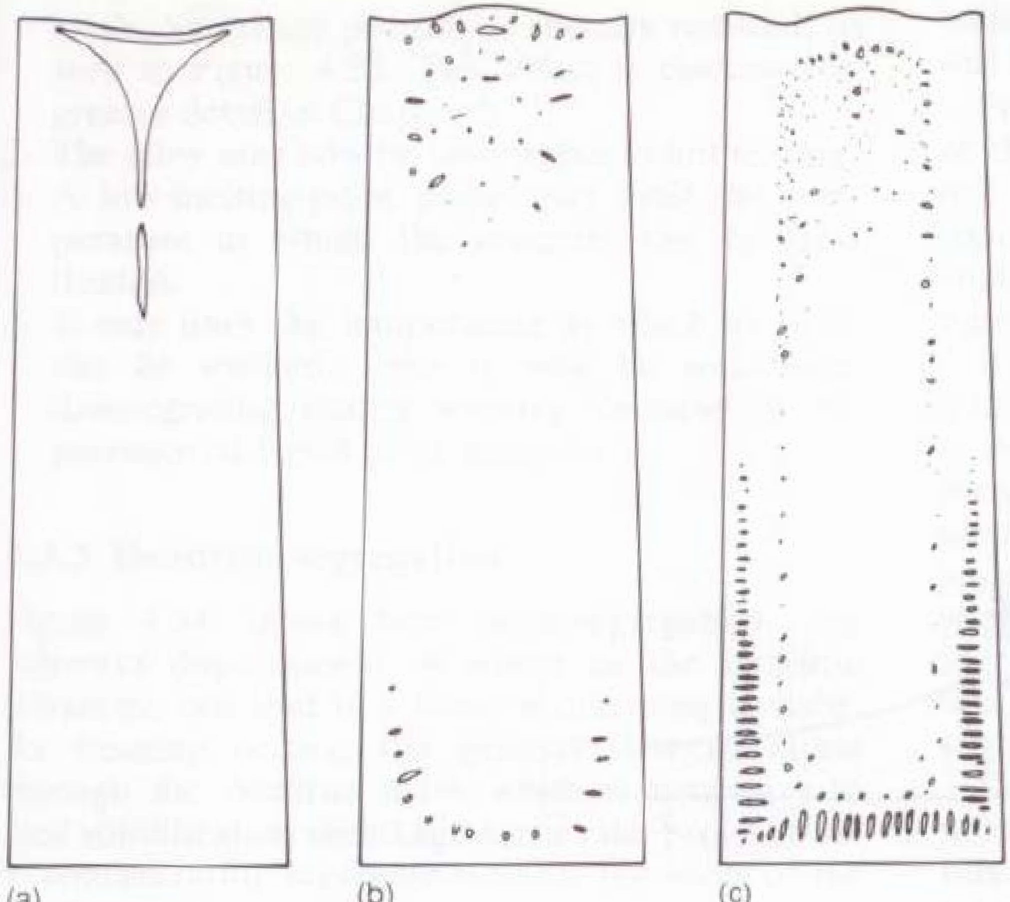

Figure 4.31 *Three ingot structures: (a) a killed steel; (b) a balanced steel; and (c) a rimming steel.*

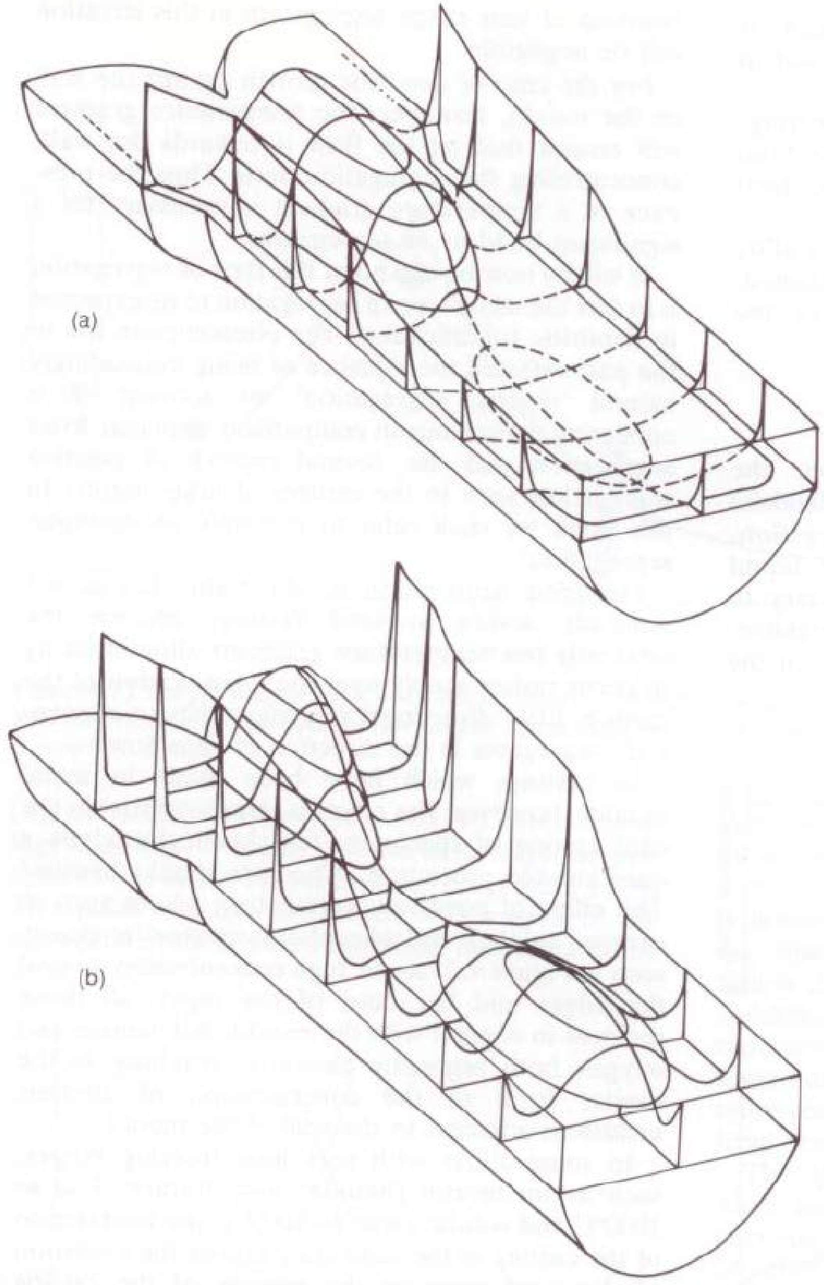

Figure 4.35 *The segregation of (a) solutes and (b) inclusions in a 3000-kg sand cast ingot. Information mainly from Nakagawa and Momose (1967).*

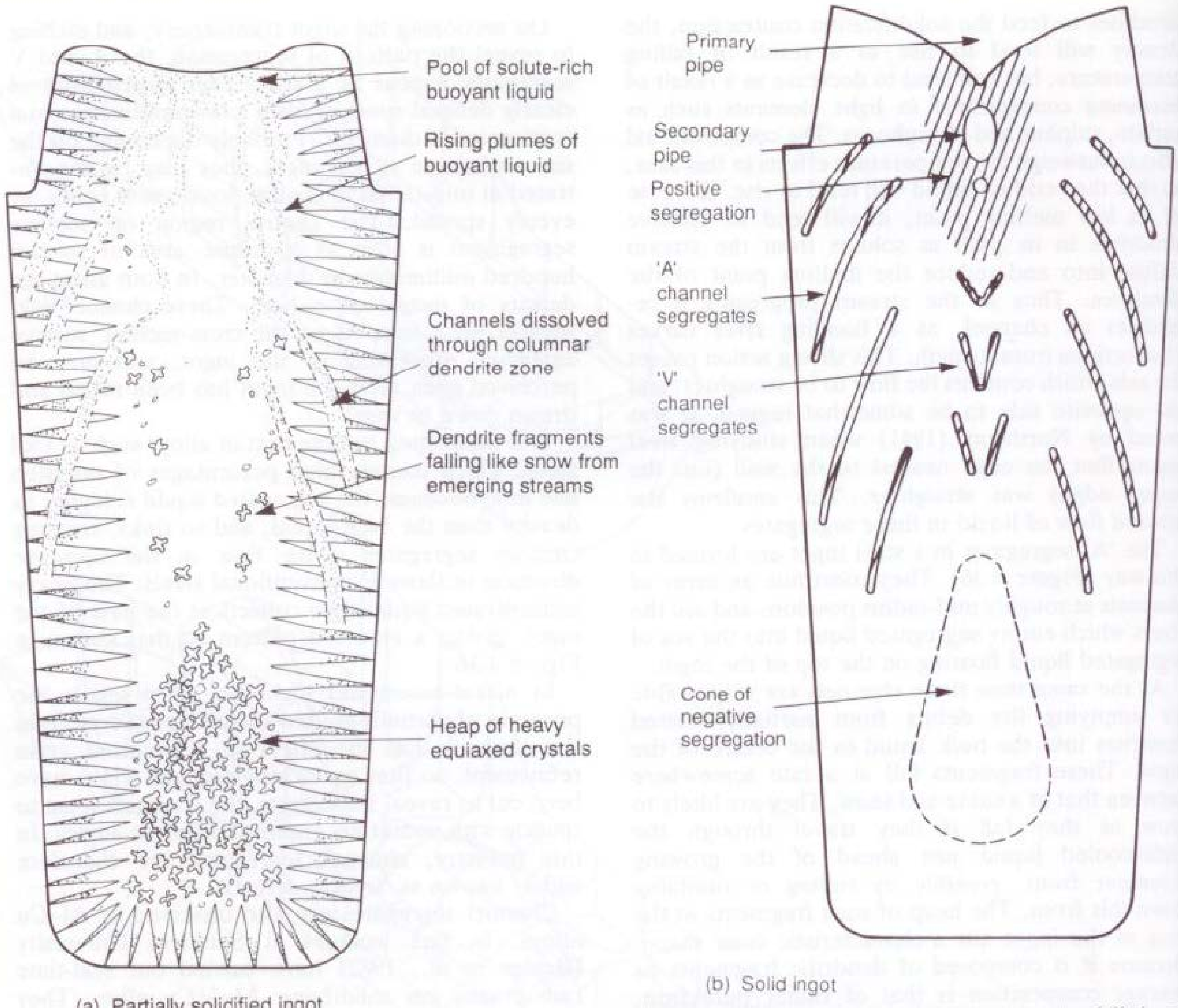

Figure 4.36 *The development of segregation in a killed steel ingot (a) during solidification and (b) in the final ingot.*

Gamma loop

Lesley Cornish

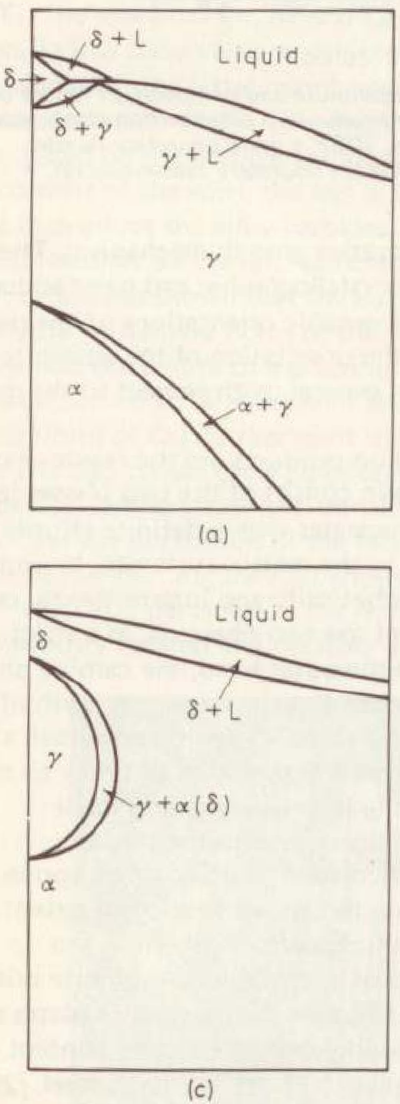

Figure 7.78 Different types of iron-based phase diagrams. (a) Open γ-phase field; Mn, Ni, Co. *(b) Expanded but limited γ-phase field;* Cu, Zn, Au, N, C. *(c) Closed γ-phase field;* Si, Cr, W, Mo, P, V, Ti, Be, Sn, Sb, As, Al. *(d) Contracted γ-phase field;* Ta, Zr, B, S, Ce, Nb

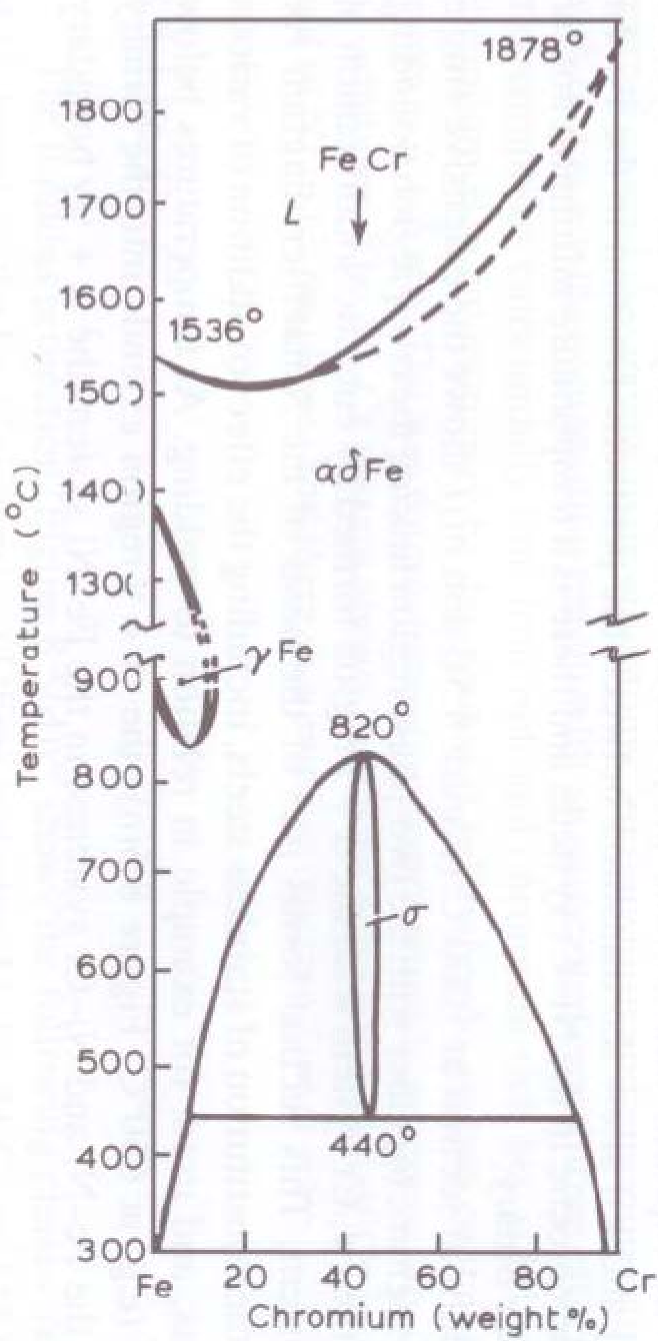

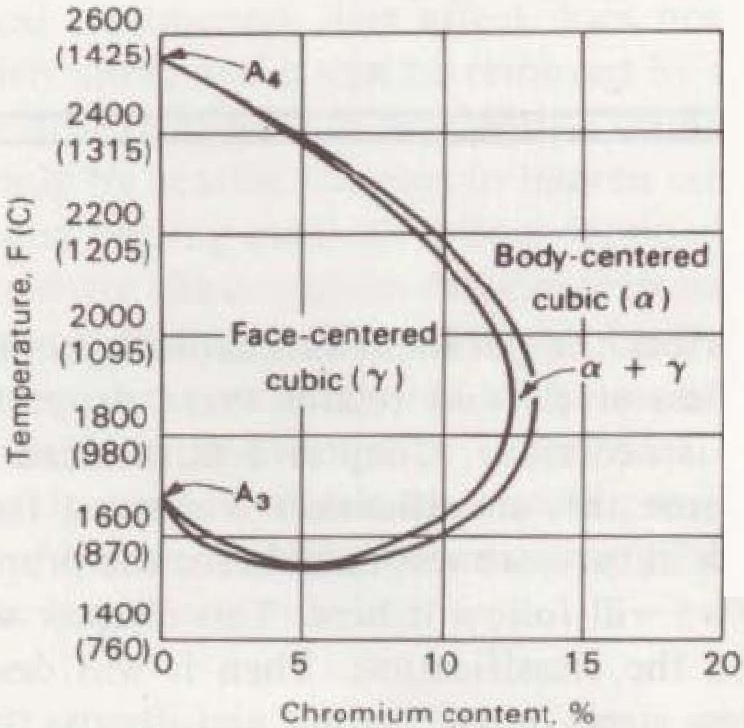

Fig. 4.1. Partial iron-chromium phase diagram.

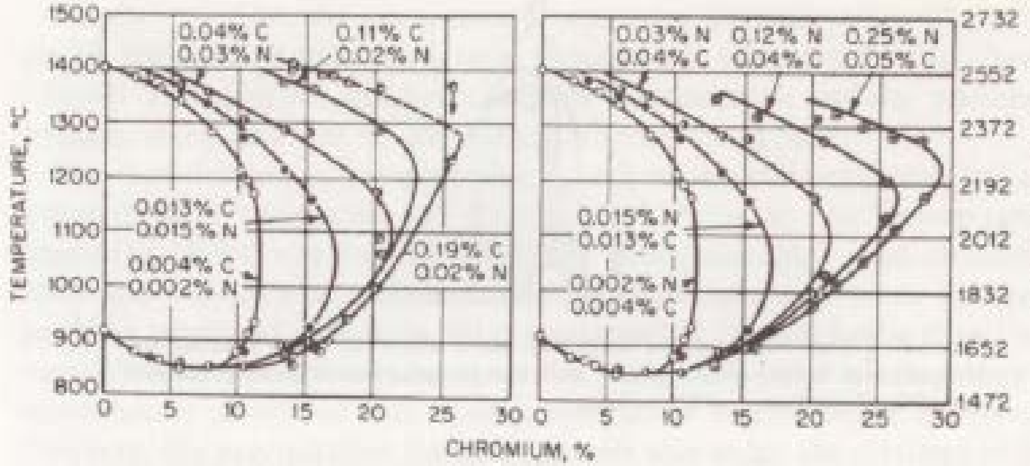

Fig. 4.2. Shifting of the boundary line $(\gamma + \alpha)/\alpha$ in the Cr-Fe system through increasing additions of carbon or nitrogen.

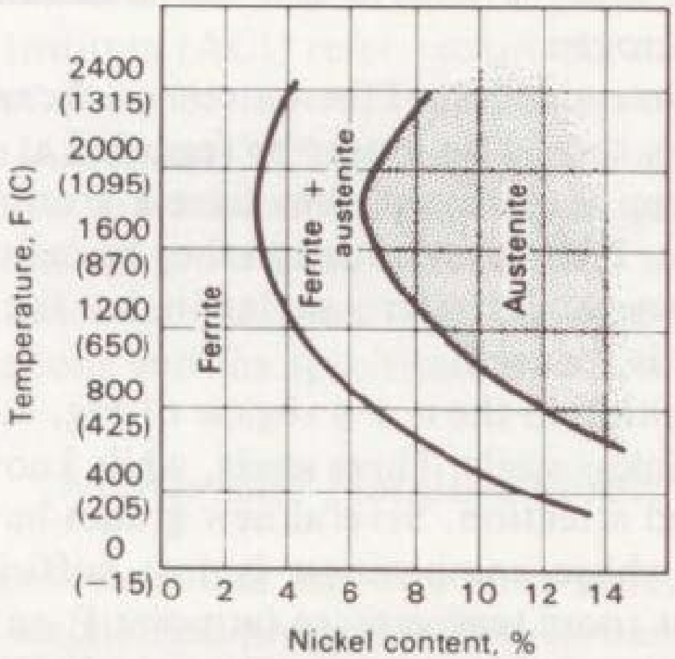

Fig. 4.3. Effect of nickel content on the stability of austenitic in an iron alloy containing 18% chromium.

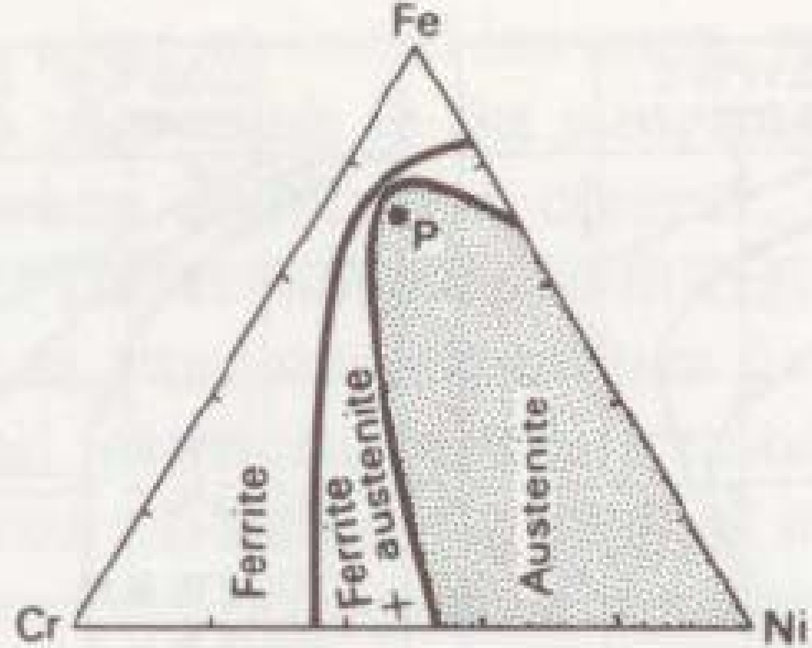

Fig. 4.4. Compositions of iron-chromium-nickel alloys for which austenite persists at room temperature. Point P indicates the position of an alloy containing 18% chromium and 8% nickel.

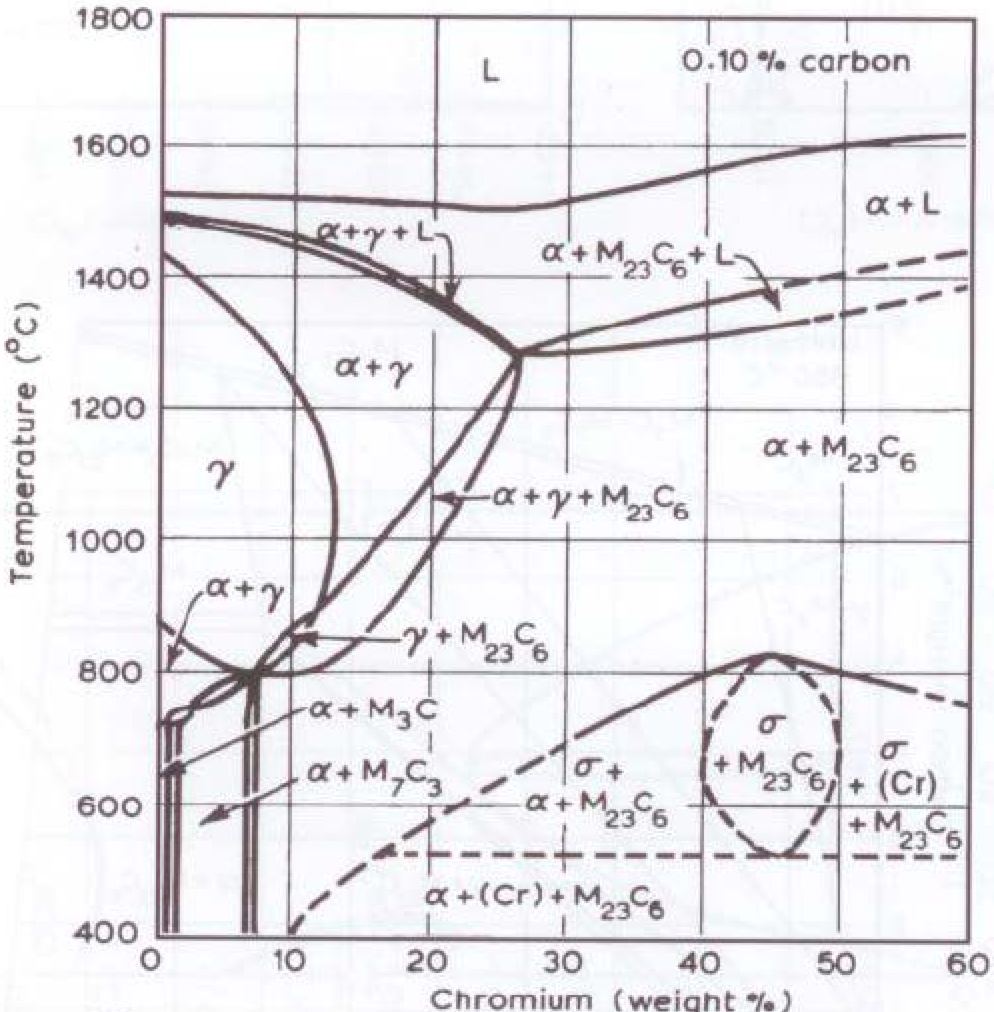

(g)

Fig. 8.5 Fe–Cr–C system (f) Isothermal section at 700°C and (g) Vertical section at 0.10% C. The diagram (Ref.42) has been modified here to agree with the form obtained by a CALPHAD calculation in the solid state region to show the invariant reaction at ~510°C involving σ, α, (Cr) and $M_{23}C_6$. (d to g.[42] Metals Handbook, 8th Edition. Reproduced with permission from ASM International, Materials Park, OH 44073-0002, USA).